Field-free molecular alignment for probing collisional relaxation dynamics

Th. Vieillard,[1] F. Chaussard,[1] F. Billard,[1] D. Sugny,[1] O. Faucher,[1] S. Ivanov,[2] J.-M. Hartmann,[3] C. Boulet,[4] and B. Lavorel[1]

[1]*Laboratoire Interdisciplinaire Carnot de Bourgogne (ICB), UMR 6303 CNRS-Université de Bourgogne, BP 47870, F-21078 Dijon Cedex, France*

[2]*Institute on Laser and Information Technologies of Russian Academy of Sciences (ILIT RAS), Advanced Laser Technology Department 2 Pionerskaya Street, Troitsk, 142190, Moscow, Russia*

[3]*Laboratoire Interuniversitaire des Systèmes Atmosphériques (LISA), UMR 7583 CNRS, Université Paris Est Créteil, Université Paris Diderot, Institut Pierre-Simon Laplace, Université Paris Est Créteil, F-94010 Creteil Cedex, France*

[4]*Institut des Sciences Moléculaires d'Orsay (ISMO), UMR 8214 CNRS, Université Paris-Sud, Bt. 350, F-91405 Orsay, France*

We report the experimental study of field-free molecular alignment in CO_2 gas mixtures induced by intense femtosecond laser pulses in the presence of collisional processes. We demonstrate that the alignment signals exhibit specific features due to nontrivial collisional propensity rules that tend to preserve the orientation of the rotational angular momentum of the molecules. The analysis is performed with a quantum approach based on the modeling of rotational J- and M-dependent state-to-state transfer rates. The present work paves the way for strong-field spectroscopy of collisional dynamics.

PACS number(s): 37.10.Vz, 34.50.Ez, 42.50.Md

I. INTRODUCTION

Manipulating external degrees of freedom of molecules by intense laser fields is recognized as an important subject with stimulating perspectives in various fields such as control of chemical reactions, high-order-harmonics generation and attosecond physics [1,2], strong field ionization [3,4], strong fields molecular processes [5,6], laser filamentation [7], and more generally, study of direction-dependent interactions, to mention but a few. For all these fields, field-free molecular alignment plays a key role. So far, numerous theoretical and experimental [8,9] studies have focused on short-pulse-induced alignment in the isolated molecule limit, that is to say, in the low molecular gas density regime, while little has been done for aligning molecules in the high-density range. However, so as to deal with more realistic experimental conditions, it is necessary to account for environmental effects, in particular those induced by intermolecular collisions.

While the effects of the gas density on alignment dynamics have received little experimental attention [10,11], some theoretical works have included the collisional relaxation in alignment models, following different ways. In this scope, the pioneer work of Ramakrishna and Seideman [12–14] remained for long the only detailed analysis on the subject. It consists in a theory of nonadiabatic alignment using a quantum-mechanical density matrix formalism in which the effects of collisions are treated through rotational state-to-state rates calculated within the so-called energy-corrected sudden (ECS) approximation. In these works, the rates were supposed independent on the M magnetic quantum number, which is the projection along the polarization axis of the total angular momentum $\vec{J}$ vector, and the effects of M-changing and J-conserving elastic collisions were neglected. The authors recommended interesting outlooks by highlighting the ability of using high-density studies to get independent information on rotational population relaxation and pure-phase decoherence effects, imperfectly known with the standard classical methods. They also underlined that there could be an interest in taking advantage of the dissipative dynamics for increasing the alignment lifetime. Recently, a similar quantum approach but with J- and M-dependent state-to-state rates of both elastic and inelastic collisions has been proposed [15]. It has been applied to pure CO_2 molecules and compared with totally independent classical molecular dynamics simulations. The results of both models are in remarkable agreement and show a noticeable propensity of collisions to conserve the ratio M/J, in contradiction with the assumption made in Ref. [14] of M-independent state-to-state rates. The theoretical analysis of Ref. [15] shows that the fact that the orientation of J is partially conserved during collisions impacts the dynamics of the field-free alignment. Only a thorough experimental study can confirm which one of the above relaxation models is valid. So far, only two experimental works dealing with the influence of collisional processes on molecular alignment have been reported. In Ref. [10], the model proposed in Ref. [14] has been applied to experimental data, but the pressure range which was studied remained too low to enable a satisfactory test of the relaxation model, and the determination of the damping of rotational coherence in N_2-X mixtures performed in Ref. [11] offered no comparison with theoretical predictions.

Thus, in this article, we report the determination of two significantly different collision-induced decays of field-free molecular alignment resulting from M/J conserving collisions, thanks to the use of high pressures and field intensities. Not only the case of pure CO_2 is investigated, but the role of He as a different buffer gas is also highlighted: we show, for instance, that the above effect is larger in the case of CO_2-He mixtures. By confronting both approaches presented in Refs. [14,15], the present work unambiguously assesses the appropriate model to be used for modeling alignment in applications where relaxation phenomena play an important role.

II. THE MODEL

Very few theoretical ingredients of the approach used here will be recalled, inasmuch as it is that presented in

Refs. [14,15]. So as to account for the environmental effects, it is relevant to use the framework of the density operator $\rho(t)$. It enables the calculation of the expectation value of the squared cosine of the angle θ between the molecule axis and the $\vec{z}$ axis of polarization of the excitation field (characterizing the alignment of the ensemble of molecules) as follows:

$$\langle \cos^2 \theta(t) \rangle = \sum_{J,M,J',M'} \rho_{JM,J'M'}(t) \langle J'M' | \cos^2 \theta | JM \rangle. \quad (1)$$

Using the $\Delta J = 0, \pm 2$, $\Delta M = 0$ selection rules of $\cos^2 \theta$, the previous equation can be split into "transient" and "permanent" contributions given by

$$\langle \cos^2 \theta(t) \rangle_{\mathrm{T}} = \sum_{J,M,J'=J\pm 2} \rho_{JM,J'M}(t) \langle J'M | \cos^2 \theta | JM \rangle$$

$$\langle \cos^2 \theta(t) \rangle_{\mathrm{P}} = \sum_{J,M} \rho_{JM,JM}(t) \langle JM | \cos^2 \theta | JM \rangle, \quad (2)$$

with $\rho_{JM,J'M}(t)$ the coherence between $|JM\rangle$ and $|J'M\rangle$, and $\rho_{JM,JM}(t)$ the population of the $|JM\rangle$ state. When the molecules are randomly oriented, $\langle \cos^2 \theta(t) \rangle_{\mathrm{T}}$ and $\langle \cos^2 \theta(t) \rangle_{\mathrm{P}}$ are equal to 0 and 1/3, respectively. Through the laser pulse interaction, a coherent superposition of rotational levels is created, leading to a value of $\langle \cos^2 \theta(t) \rangle_{\mathrm{P}}$ greater than 1/3, depending on the laser intensity. Meanwhile, $\langle \cos^2 \theta(t) \rangle_{\mathrm{T}}$ reaches nonzero values which oscillate at the rotational period [16]. This alignment is preserved as long as the coherence is maintained. When collisional mechanisms take place (as the gas density increases), coherences are destroyed and populations relax; therefore $\langle \cos^2 \theta(t) \rangle_{\mathrm{T}}$ and $\langle \cos^2 \theta(t) \rangle_{\mathrm{P}}$ decrease more or less slowly down to their equilibrium value. These behaviors are described through the time evolution of the density operator $\rho(t)$, which obeys the Bloch-Redfield form of the Liouville–von Neumann equation [14,17]:

$$\frac{d\rho}{dt}(t) = -\frac{i}{\hbar}[H_0 + H_{\mathrm{L}}(t), \rho(t)] + \left(\frac{d\rho(t)}{dt}\right)_{\mathrm{coll}}, \quad (3)$$

where H_0 is the free rotational Hamiltonian, $H_{\mathrm{L}}(t) = -\frac{1}{2}(\alpha_\parallel - \alpha_\perp)E^2(t)(\cos^2 \theta - \frac{1}{3})$ is the interaction Hamiltonian limited to the angle-dependent term of the potential, $\alpha_\parallel - \alpha_\perp$ is the anisotropy of polarizability, and $E(t)$ is the amplitude of the linearly polarized electric field. As in Refs. [14,15,18], the effects of intermolecular collisions are treated with the Bloch model within the Markov and secular approximations, which make use of the rates of population transfer from state $|JM\rangle$ to state $|J'M'\rangle$. The latter directly drive the time constants of the above-described decreases of $\langle \cos^2 \theta(t) \rangle_{\mathrm{P}}$ and $\langle \cos^2 \theta(t) \rangle_{\mathrm{T}}$. At this point, the difference between [14,15] relies on the modelization of those rates, and will be referred to as the ECS M-independent and ECS M-dependent models, respectively. Indeed, both works make use of the ECS scaling law, extensively used in literature and successfully applied to frequency-resolved studies to describe the spectral effects of line-mixing processes [19]. It should be pointed out that IR and Raman spectroscopy have shown that ECS is particularly relevant in the case of a linear molecule like CO_2 with a small rotational constant, and in the pressure range investigated here [19]. A detailed description of this scaling law can be found in Refs. [14,15].

The calculations of the alignment dynamics were performed by including CO_2 levels up to $J = 100$, using the values $\alpha_\parallel = 30.1$ a.u. and $\alpha_\perp = 14.7$ a.u. [20,21], and the ECS parameters given in Refs. [15,22] for CO_2-CO_2 and CO_2-He collisions, respectively. A time step of 2 fs was retained to solve Eq. (3), and the variation of the (linearly polarized) laser power during the pulse was represented by a Gaussian function of 100 fs FWHM.

For quantitative comparisons with experimental data, the two components in Eq. (2) are used to calculate the so-called homodyne signal proportional to

$$[\langle \cos^2 \theta(t) \rangle_{\mathrm{P}} + \langle \cos^2 \theta(t) \rangle_{\mathrm{T}} - 1/3]^2. \quad (4)$$

This numerical result is then convoluted with a Gaussian function representing the probe pulse temporal intensity. Finally, the simulations are fitted to the experiments by adjusting an appropriate scale factor and an effective pump peak intensity around its experimental value for the best agreement with the observed shapes of the transients. The degree of alignment is thus determined through the shape of the signal and not through the amplitude which would require calibrated measurements. It is worth mentioning that this effective intensity takes roughly into account the volume effect, that is to say, the spatial dependence of the electric fields for the beams, which is not included in the calculations for saving computational time. Indeed, a previous study [23] showed that taking the averaged measured intensity of the incoming beam allows a satisfactory match between theory and experiment.

III. EXPERIMENT

Since the experimental setup was described in detail previously [10], only the important features are recalled here. Briefly, the time evolution of the alignment is measured thanks to the orientational contribution to the optical Kerr effect based upon the modification of the polarization of a probe beam by the studied medium [16]. Among other advantages, the method can be applied at high pressure. The incoming beam, provided by a Ti-sapphire chirped-pulse amplified laser system operating at 1 kHz (pulse duration 100 fs), is split into two parts: the stronger one is used as the pump, whereas the weaker one, time delayed with respect to the former, is used as the probe. Both pulses are linearly polarized at 45° to each other. The probe is frequency doubled so as to be correctly filtered out from the scattering of the pump by the cell windows and the gas. The pump and probe beams being crossed with a small angle in the gas sample, a loss of temporal resolution is generally observed. A practical way to account for this effect in the calculations is to assign to the probe pulse duration a higher value than expected from pulse duration measurements (130 fs instead of 100 fs). Because of the high pressures (from 2 up to 30 bar) studied here, the static cell has been designed in order to limit the appearance of any additional static birefringence due to mechanical constraints in its sapphire windows that would hence heterodyne the signal.

IV. RESULTS AND DISCUSSION

We have investigated the field-free alignment of CO_2 in CO_2–X ($X = CO_2$, He) mixtures from low to high pressures
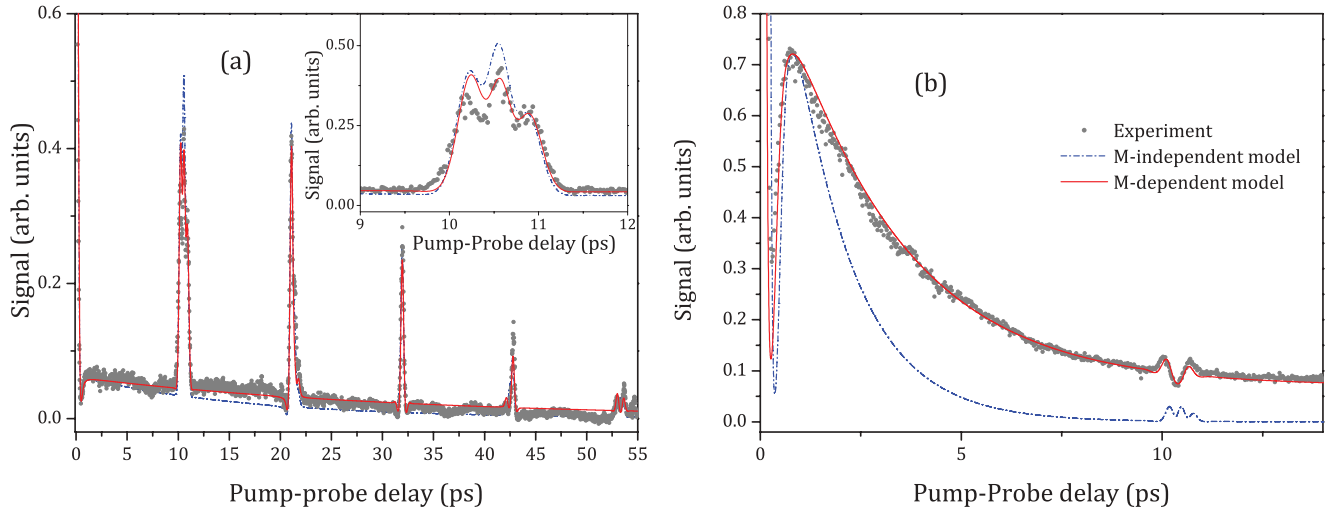
FIG. 1. (Color online) Experimental homodyne signal (gray dotted curves) as a function of the pump-probe delay in pure CO_2 at 295 K and comparisons with numerical simulations using the M-independent (blue dash-dotted curves) and M-dependent quantum ECS model (solid red curves): (a) 2 bar with a peak intensity of 45 TW/cm^2 and (b) 20 bar with a peak intensity of 35 TW/cm^2. The inset in (a) shows the shape of the first transient.

($2 \leqslant P \leqslant 30$ bar) at 295 K. Figure 1 displays the comparisons between measured and calculated alignment traces for pure CO_2. According to Eqs. (3) and (4), the observed signal consists of equally spaced (by a quarter of the classical rotational period) transients or revivals. They appear with a multiple-peaks structure corresponding to an alternation of alignment (when $\langle \cos^2 \theta(t) \rangle_T > 1/3$) and planar delocalization in a plane perpendicular to the pump polarization (when $\langle \cos^2 \theta(t) \rangle_T < 1/3$) [24]. The nonzero background signal between these revivals corresponds to the permanent alignment of the molecules arising from $\langle \cos^2 \theta(t) \rangle_P$. For a sufficiently large gas density, a damping of the signal is observed, with the two components $\langle \cos^2 \theta(t) \rangle_T$ and $\langle \cos^2 \theta(t) \rangle_P$ exhibiting different monotonic decays. This has been evidenced by fitting the permanent component $[\langle \cos^2 \theta(t) \rangle_P - 1/3]^2$ in each trace with an exponential law, yielding normalized time constants per unit pressure. For reliable determinations of the associated uncertainties, this procedure has been applied to about 90 alignment recordings between 5 and 20 bar. As for the decay of the transient component, the integrated peak areas of the revivals have been used, as done in Ref. [11], and plotted as a function of the temporal delay. A single exponential least-squares fit was then performed, from which another normalized time constant was derived. Three alignment recordings at 2 bar (five revivals) were used. The corresponding results are collected in Table I. The fast decay of the transient component (73 ps atm^{-1}) as compared to the permanent one (127 ps atm^{-1}) is analyzed by means of the ECS simulations provided in Fig. 1. At low pressure, both ECS M-dependent and independent models reproduce quite well the behavior of the permanent component, but a discrepancy can be observed when reproducing the transient amplitudes, as shown thanks to the inset in Fig. 1(a). Yet noticeable, this discrepancy may not be significant enough to discriminate the two models. It explains the conclusions brought by Ref. [10]: because of the too-low investigated pressures and the absence of comparison with an alternative model, the discrepancy was

attributed to the weak effect of elastic dephasing (J and M conserving) collisions. On the other hand, at high pressure [see Fig. 1(b)] it is obvious that the ECS M-independent model completely fails to reproduce the experimental data, by strongly underestimating the decay time of the permanent component, while the M-dependent approach matches well the experiments. The predictions of the M-dependent and M-independent quantum ECS models for the normalized time constants are reported in Table I. As can be seen, the M-dependent ECS approach is in good agreement with the measurements, while the M-independent assumption largely fails in representing the behavior of the permanent component. As predicted in Ref. [15], the permanent component is mainly sensitive to inelastic collisions, the reorienting elastic collisions representing only 10% of the total relaxation rate. The observed slower decay of the permanent component of the alignment than expected when assuming that collisions fully randomize the orientation of the angular momentum confirms that the ratio M/J is significantly conserved through inelastic collisions. On the contrary, the transient component is sensitive to both elastic and all inelastic collisions. But in this case, the M/J conserving property plays no role, since coherences are destroyed all the same whatever the collision. Therefore the transient component decays faster than the permanent one.

TABLE I. Decay times in ps.atm^{-1} of the exponential decays of the permanent and transient components of $\langle \cos^2 \theta \rangle$ predicted by the ECS models, and experimental determinations. The numbers in parenthesis correspond to one standard deviation.

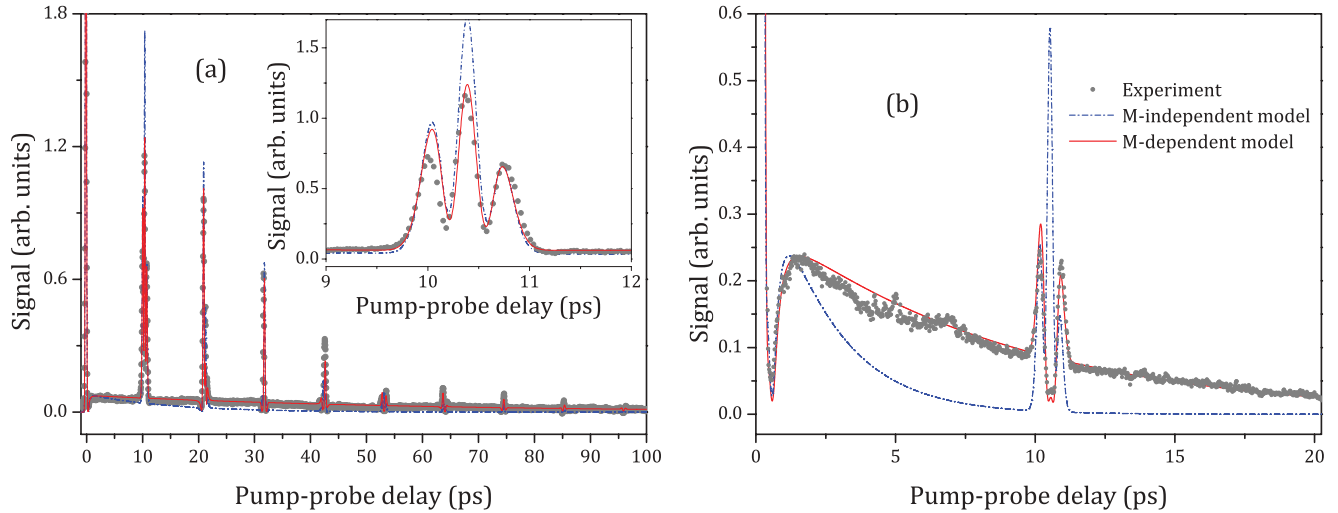| Model	Pure CO_2		10% CO_2-90% He	
	Permanent	Transient	Permanent	Transient
Expt.	127(10)	73(7)	403(42)	88(9)
ECS M-dep.	126	57	343	75
ECS M-indep.	66	64	90	89

FIG. 2. (Color online) Same as Fig. 1 but in CO_2 (10%)-He (90%) mixtures: (a) 3 bar with a peak intensity of 35 TW/cm^2 and (b) 20 bar with a peak intensity of 20 TW/cm^2. The inset in (a) shows the shape of the first transient.

The above effect is not restricted to molecule-molecule collisions. It also occurs in atom-molecule collisions, as demonstrated here with the investigation of CO_2-He mixtures. The results plotted in Fig. 2 have been obtained with 10% CO_2 and 90% He mixtures, providing a good enough signal-to-noise ratio while keeping large effects of the buffer gas. The corresponding decay time constants are presented in Table I. A comparison of the two gases shows that although the transient decay times are similar, the permanent component exhibits a much slower decay in the case of the gas mixture: the experimental ratio of the decay times of the permanent and transient components of the alignment is about 4.6 for CO_2-He and about 1.7 for pure CO_2. These numbers are well reproduced by the M- and J-dependent ECS model but not by the M-independent assumption. The slower decrease of the permanent component results from a stronger propensity of CO_2-He collisions to conserve the orientation of the angular momentum due to conjugative effects of the reduced mass and the potential range. It also explains the changes observed on the shape of the first transient shown in Fig. 2(b) as compared to Fig. 1(b). According to Eq. (4), the structural shape of the transient features is driven by the respective amplitudes of $\langle \cos^2 \theta(t) \rangle_P$ and $\langle \cos^2 \theta(t) \rangle_T$. The larger value of the former in CO_2-He due to a much slower decay (403 ps.atm^{-1}) as compared to CO_2 (127 ps.atm^{-1}) leads to a stronger signal modulation around the first transient (10.6 ps).

V. CONCLUSION

A thorough analysis of the dissipative decay of laser-induced field-free molecular alignment produced under large pressure conditions has enabled us to get beneficial information about the effects of collisions, which until now have not been retrieved using conventional spectroscopic methods. The higher-than-expected value (following Ref. [14]) of the permanent alignment decay time measured in the present work demonstrates a strong propensity of inelastic collisions to conserve the angular momentum orientation (i.e., M/J), as predicted in Ref. [15]. Although this is foreseen in the classical mechanical description of colliding tops, it has never been evidenced for quantum rotors. This study calls for a proper description of M-changing collisions, as previously theoretically proposed in Ref. [15] for pure CO_2, and concomitantly extends the result to gas mixtures. Besides supporting the idea that field-free alignment can provide unique information about dissipative environments and help in discriminating pure dephasing collisions from other collisions, as proposed in precursory papers of Ramakrishna and Seideman [12–14], the present work also prefigures new approaches for investigating collision dynamics with strong-field spectroscopy.

[1] J. Itatani, D. Zeidler, J. Levesque, M. Spanner, D. M. Villeneuve, and P. B. Corkum, Phys. Rev. Lett. **94**, 123902 (2005).

[2] S. Haessler, J. Caillat, W. Boutu, C. Giovanetti-Teixeira, T. Ruchon, T. Auguste, Z. Diveki, P. Breger, A. Maquet, B. Carr *et al.*, Nat. Phys. **6**, 200 (2010).

[3] S. K. Lee, Y. F. Lin, L. Yan, and W. Li, J. Phys. Chem. A **116**, 1950 (2012).

[4] J. L. Hansen, L. Holmegaard, J. H. Nielsen, H. Stapelfeldt, D. Dimitrovski, and L. B. Madsen, J. Phys. B **45**, 8 (2012).

[5] S. M. Purcell and P. F. Barker, Phys. Rev. A **82**, 033433 (2010).

[6] E. Gershnabel and I. S. Averbukh, J. Chem. Phys. **135**, 084307 (2011).

[7] J. Wu, H. Cai, Y. Peng, Y. Q. Tong, A. Couairon, and H. P. Zeng, Laser Phys. **19**, 1759 (2009).

[8] T. Seideman and E. Hamilton, Adv. At., Mol., Opt. Phys. **52**, 289 (2006).

[9] H. Stapelfeldt and T. Seideman, Rev. Mod. Phys. **75**, 543 (2003).

[10] T. Vieillard, F. Chaussard, D. Sugny, B. Lavorel, and O. Faucher, J. Raman Spectrosc. **39**, 694 (2008).

[11] N. Owschimikow, F. Konigsmann, J. Maurer, P. Giese, A. Ott, B. Schmidt, and N. Schwentner, J. Chem. Phys. **133**, 044311 (2010).

[12] S. Ramakrishna and T. Seideman, J. Chem. Phys. **122**, 084502 (2005).

[13] S. Ramakrishna and T. Seideman, Phys. Rev. Lett. **95**, 113001 (2005).

[14] S. Ramakrishna and T. Seideman, J. Chem. Phys. **124**, 034101 (2006).

[15] J.-M. Hartmann and C. Boulet, J. Chem. Phys. **136**, 184302 (2012).

[16] V. Renard, M. Renard, S. Guérin, Y. T. Pashayan, B. Lavorel, O. Faucher, and H. R. Jauslin, Phys. Rev. Lett. **90**, 153601 (2003).

[17] W. K. Liu and R. A. Marcus, J. Chem. Phys. **63**, 272 (1975).

[18] V. May and O. Kuhn, *Charge and Energy Transfer Dynamics in Molecular Systems* (Wiley, Weinheim, 2004).

[19] J.-M. Hartmann, C. Boulet, and D. Robert, *Collisional Effects on Molecular Spectra: Laboratory Experiments and Models, Consequences for Applications* (Elsevier, Amsterdam, 2008).

[20] A. P. Kouzov and M. Chrysos, Phys. Rev. A **80**, 042703 (2009).

[21] J.-M. Hartmann, C. Boulet, and D. Jacquemart, J. Chem. Phys. **134**, 094316 (2011).

[22] R. Rodrigues, B. Khalili, R. LeDoucen, L. Bonamy, and J.-M. Hartmann, J. Chem. Phys. **107**, 4118 (1997).

[23] A. Rouzée, V. Renard, B. Lavorel, and O. Faucher, J. Phys. B **38**, 2329 (2005).

[24] V. Renard, M. Renard, A. Rouzée, S. Guérin, H. R. Jauslin, B. Lavorel, and O. Faucher, Phys. Rev. A **70**, 033420 (2004).